DENSE: Displacement Encoding with Stimulated Echoes in Cardiac Functional MRI

Anthony H. Aletras, **Shujun Ding**, **Robert S. Balaban**, and **Han Wen**
Laboratory of Cardiac Energetics, NHLBI, NIH, Bethesda, Maryland 20892-1061

Abstract

Displacement encoding with stimulated echoes (DENSE) was developed for high-resolution myocardial displacement mapping. Pixel phase is modulated by myocardial displacement and data spatial resolution is limited only by pixel size. 2D displacement vector maps were generated for the systolic action in canines with 0.94×1.9 mm nominal in-plane resolution and 2.3 mm/π displacement encoding. A radial strain of 0.208 was measured across the free left ventricular wall over 105 ms during systole. DENSE displacement maps require small first-order gradient moments for encoding. DENSE magnitude images exhibit black-blood contrast which allows for better myocardial definition and reduced motion-related artifacts.

Keywords

cardiac; function; STEAM; PC; phase contrast; stimulated echoes; heart

---

In recent years magnetic resonance imaging has developed the capability to evaluate myocardial perfusion and function (1). Functional studies provide information on the contractile action of the cardiac muscle, a potential indicator of its viability (2–7). This paper introduces a phase contrast method for *d*isplacement *en*coding via *s*timulated *e*choes (DENSE) that has the ability to extract myocardial motion data at high spatial density over segments of the cardiac cycle.

To date, two categories of pulse sequences have been proposed in order to evaluate cardiac function with magnetic resonance imaging. The first relies on tagging the magnitude images with a grid of signal voids during RF excitation and subsequently tracking the tags when the signal is acquired (8–10). Such a grid can be implemented through selective saturation (8) or through modulation of the magnetization vector by gradient fields (9). Both approaches are easily applicable on standard clinical scanners. Data acquired with tagging provide information with respect to muscle deformation (2,3,9–16). While easy to visualize and implement, tagging methods suffer from low spatial resolution. The need to adequately define the saturation grid and the fact that myocardial signal is deliberately suppressed limit the resolution. Therefore, it is difficult to measure transmural variations in motion with tagging methods.

The other approach to functional cardiac imaging is through phase contrast (PC) velocity encoding of the myocardial spins (17). With this method, spins acquire phase that is proportional to their velocity. This is achieved through the application of bipolar gradient lobes along the desired direction prior to signal acquisition. Since the phase of a pixel is modulated by velocity, one can attain functional data with maximum resolution since each pixel contains velocity data (18–21). However, short periods of motion are recorded with PC velocity encoding. To encode low velocities, larger first-order gradient moments have to be applied. This results in prolonged echo times and phase distortion. The latter is a direct manifestation of eddy currents and Maxwell terms. Gradient system performance is critical in accurately

extracting velocity information with PC methods. Moreover, additional phase distortion due to cardiac motion in areas of high susceptibility boundaries further degrades data quality. Such susceptibility interfaces are found in the posterior left ventricular wall.

Combining the advantages of both tagging and phase velocity mapping methods has the potential of yielding a method capable of measuring large displacements over long periods while maintaining high spatial resolution. Recently, such results pertaining to magnetic resonance elastography were presented through manipulation of the spin phase in a stimulated echo imaging experiment (22). In an effort to quantify displacement resulting from deformation induced by external forces, the phase of each pixel was modulated according to its position rather than its velocity.

Based on the same principle, a *d*isplacement *en*coding *s*timulated *e*cho method was developed to provide a high spatial density of displacement measurements in the myocardium via stimulated echoes. This technique encodes motion over long time intervals. The encoded displacements are large; therefore, improved phase contrast is obtained with moderate gradient strength. In this paper we present the details of this technique and preliminary results obtained with DENSE from canines *in vivo*.

To encode displacement over a time comparable to T_1 the magnetization vector must be stored along the direction of the static magnetic field to avoid T_2^*-related signal decay. This was accomplished with stimulated echoes.

The basic pulse sequence is schematically presented in Fig. 1. After an initial RF excitation, phase dispersion was introduced with a single gradient lobe along the desired direction. For example, along the read direction the gradient pulse was set at G_5 G/cm and duration t_{enc}. Subsequently, a second RF pulse was applied to preserve the magnetization along the longitudinal axis. Displacement was encoded during a long mixing period TM followed by a third RF pulse that brought the magnetization onto the transverse plane. There, a second gradient pulse of amplitude G_6 (where $G_5 = G_6$) rewound the phase dispersion from the first lobe. For stationary spins this phase rewinding was complete. For spins that had moved Δx between G_5 and G_6 along the read direction, a phase of $\varphi_1 = \gamma_{\mathrm{H}} G_5 t_{\mathrm{enc}} \Delta x$ was accumulated. Imaging was performed with slice selection during the third RF pulse followed by sequential *k*-space sampling at one view per excitation. The sequence was repeated once more with altered amplitude of the position sensitizing gradient pulses (where $G_5^* = G_6^*$). The phase accumulated was then $\varphi_2 = \gamma_H G_5^* t_{\mathrm{enc}} \Delta x$. The phase difference between the images was $\Delta\varphi = \gamma_H t_{\mathrm{enc}}(G_5 - G_5^*)\Delta x$. This equation was used to measure Δx. Other phase contributions common to both images were canceled. Since Δx occurred over-approximately 100 ms large phase differences $\Delta\varphi$ were obtained with moderate encoding gradient pulses. To measure displacement along the read and slice directions, the corresponding encoding gradient amplitudes were modified accordingly.

All experiments were performed on a 4-T Oxford magnet (Oxford, England) equipped with a whole-body three-axis gradient set capable of 1.3 G/cm. Signal was acquired with a Surrey Medical Imaging Systems console (Surrey, England) outfitted with a digital receiver and digital gradient driver boards. A quadrature transmit/receive coil of 27 cm in diameter (23) was utilized for excitation/reception.

In vivo displacement data from beagles were collected to study the contraction of the heart. The animals were externally ventilated and the cardiac muscle was paced to an integer multiple of the respiratory frequency. Following a cardiac-triggered fast gradient echo sagittal localizer, short-axis planes (slice thickness of 5 mm) were prescribed with DENSE. Care was taken to ensure that the heart was located at isocenter. One view per external respiratory triggering pulse

was sampled at 100 kHz. The matrix size was set to 256×128 for a field of view of 240×240 mm. The TM period was gated to occur over the 105 ms before end systole. This allowed for measurement of systolic displacement. Image acquisition at end systole was used to maximize wall thickness and improve transmural spatial resolution. In order to account for through-plane motion, the first two RF excitations were performed with nonselective 600-µs pulses. Due to the long TR period dictated by the respiratory triggering process, the slice-selective sinc RF pulse following the TM period was 90°. The magnetization vector remained in the transverse plane for a total period of TE = 6 ms. During that time, displacement encoding gradients (Fig. 1) along the required axis were applied at gradient strengths of 0.3, 0.9, and 0.15 G/cm for the slice (G_1, G_2), read (G_5, G_6), and phase (G_3, G_4) axes, respectively (plateau = 500 µs, ramp = 600 µs). The maximum first-order moment of the Z gradient direction was kept at 840 µs*G/cm to keep signal loss due to through-slice contraction low. The second displacement sensitizing gradient pulses (G_2, G_4, G_6) also served as means of dispersing the FID signal following the slice-selective RF pulse. The TM period was set to 105 ms. Crusher gradients (G_7–G_9) at 0.75 G/cm (30 ms in duration) were applied during TM to suppress signal not pertaining to the stimulated echo experiment. Crushers were also applied at the end of each TR period along the read and slice axes.

The stimulated echo imaging sequence was repeated a total of four times to acquire displacement encoded short-axis data from a midventricular slice of the heart. The first repetition served as a reference scan. Each of the remaining three repetitions was carried out with a modified amplitude of the displacement encoding gradient along a specific direction. The first moment of the difference between the gradient pulses of the reference scan and each of the remaining sets was set for a 2.3mm/π displacement encoding. The difference phase maps between such a data set and the reference scan yielded information pertaining to the displacement of the cardiac muscle along a given direction.

Static phantom displacement maps were collected from an agar phantom (8 cm diameter) with imaging parameters similar to those used for the *in vivo* studies. These maps were utilized in order to evaluate baseline phase errors arising from inadequate gradient performance with respect to eddy current suppression. The phantom was located at isocenter in order to map phase errors at the same location where the *in vivo* experiments were performed.

Raw data were processed with IDL (Research Systems, Inc., Boulder, CO) to produce phase maps. Knowing the duration and amplitude of the displacement encoding gradient pulses, the phase differences were converted to displacement vectors. To correct bulk translational motion of the heart, a region of interest (ROI) was defined to include both the left and the right ventricles. The average displacement vector of all pixels in the ROI was calculated and subtracted from the displacement vector of each pixel.

The phase errors in all three orthogonal directions from the agar phantom are shown in Fig. 2. The 0th order phase error term recorded along the Y and Z directions does not affect cardiac motion studies since bulk motion is corrected via software. The small first-order term along X is likely due to eddy currents and represents an error of less than 3% of the full scale. This is equivalent to 0.26-mm error in displacement at the edges of the field of view for the in vivo experiments. In principle, this systematic error can be corrected during data processing. In practice, the heart is positioned at the center of the field of view, thus this error is negligible. Also, Maxwell terms were not considered as a source of phase error since the experiment was performed at isocenter (24).

Magnitude data from the reference scan are shown in Fig. 3 in short-axis format. Note the black-blood feature caused by the long TM period and ataxic motion of the blood in the ventricle.

A DENSE displacement map for in-plane motion is presented in Fig. 4a. The plot is a series of vectors representing individual pixels on a x–y position map. The vector length is scaled to the actual amount of displacement occurring over the 105-ms encoding period in systole. A more detailed view of the left ventricular free wall is shown in Fig. 4b. The displacements range from 1.8 to 3.4 mm with a gradient of displacement (i.e., radial strain) from epicardium to endocardium of 0.208 mm/mm (Fig. 5).

Through-plane motion in the same slice is shown by means of a grayscale in Fig. 6. A grayscale is used since the vectors now run in and out of the plane of the paper. The maximum scale corresponds to 4-mm displacement of myocardial spins along the long axis of the heart. Note that the least through-plane displacement occurred in the septum.

DENSE provided a high-density measure of myocardial displacement in the intact canine heart. Using the current-imaging parameters, approximately up to seven points across the free left ventricular wall were measured. This is well above conventional tagging resolution. The displacements were on the order of 1.5 mm over the 105-ms encoding period. The maximum displacement was 5.14 mm at the tip of a papillary muscle.

The contraction of this myocardial slice was not isotropic (Fig. 4). Displacement in the free wall of the left ventricle is mainly in a radial direction for systolic action. Wall deformation can be described by the radial gradient of displacement (25). A positive radial gradient of 0.208 mm/mm was measured from the epicardium to the endocardium (Fig. 5). This value of radial strain agrees with previously published data (26). In the intraventricular septum, a deviation from pure radial displacement is observed and rotational components become more prevalent. The physical location and contraction of the right ventricle likely cause this anisotropic displacement.

In principle, the SNR of the displacement measurement is limited by the image signal-to-noise ratio. The signal-to-noise ratio in the magnitude images was 17:1 as measured at the left ventricular free wall. As a result, the corresponding phase noise is 0.0588 rad. This translates to 43.1 µm of displacement uncertainty, since encoding was performed at 2.3 mm/π. As discussed earlier, systematic errors due to eddy currents and Maxwell terms were not significant in this study. Generally, these errors can be mapped and taken into account during data processing if needed.

Besides its ability to collect displacement data at high resolution, DENSE is advantageous due to its intrinsic black-blood T_1 contrast (Fig. 3). This type of image contrast is desirable in cardiac MRI studies for separating the myocardium from the ventricular cavity. Moreover, the lack of bright blood signal helps reduce motion artifacts along the phase direction.

A significant signal loss occurs with this technique due to intravoxel dephasing caused by the gradient pulses bracketing the TM period. Not only tissue deformation and rotation, but also perfusion, can contribute to the pixel intensity drop. Indeed, when the TE encoding gradients were increased in strength (data not shown) there was signal loss within the myocardial tissue due to the aforementioned reasons. Similarly, prolonging the encoding period up to 300 ms resulted in anisotropic and regional signal loss that can not be contributed to T_1, as evidenced by saturation recovery experiments with T_{REC} up to 300 ms. In either case, such effects have already been reported (27,28). It is difficult to separate the contribution of each term to the overall signal loss *in vivo*. As such, one has to experimentally balance among the need for adequate FID signal crushing, sensitivity of displacement measurements, and the intravoxel dephasing-related signal loss when considering the first-order moment of the displacement-encoding gradient pulses. Signal attenuation due to intravoxel dephasing also limits the extent of muscle deformation that can be encoded (27). Therefore, for a given encoding strength, cardiac displacement must be observed over a limited duration where such effects are not

dominant. During systole in the canine model, the empirical limit for the observation time (TM) was less than 105 ms. On the other hand, intravoxel dephasing could provide a measure of deformation by itself and further investigation is warranted.

With the current implementation, DENSE data are acquired slowly (4.3 min per image), making clinical application difficult. Agar phantom experiments showed that it is possible to compress the imaging sequence to accommodate multiple k_Y line sampling during each heartbeat by applying a train of small flip angle RF-pulses in place of the soft 90° to acquire segmented k-space data. A preliminary human heart image using stimulated echoes with a dedicated 1.5-T cardiac scanner is presented in Fig. 7. The combination of high-speed STEAM MRI (28) with DENSE encoding has the potential of yielding useful 2D displacement data from the human myocardium in 12 s. Frahm *et al.* (28) presented single-shot STEAM images of the heart *in vivo* in 1991. According to the authors, these results were SNR limited by inadequate hardware with respect to RF and gradient coil characteristics and the requirement for single-shot image acquisition. High-performance gradient sets and phased array coils specifically designed for cardiac imaging are now readily available. These technological advancements, in conjunction with image acquisition over multiple cardiac cycles, could yield high-quality fast-DENSE data. Furthermore, by varying the length of the TM period, images from different cardiac phases can be obtained while view sharing can provide additional phases of the cardiac cycle at no expense of imaging time. This approach would be desirable in breath-hold human cardiac imaging.

REFERENCE

1. Reichek N. Magn. Reson. Q 1991;7:255–274. [PubMed: 1790112]

2. Young AA, Kramer CM, Ferrari VA, Axel L, Reichek N. Circulation 1994;90:854–867. [PubMed: 8044957]

3. Young AA, Fayad ZA, Axel L. Am. J. Physiol 1996;271:H2677–H2688. [PubMed: 8997331]

4. Kramer CM, Rogers WJ, Theobald TM, Power TP, Petruolo S, Reichek N. Circulation 1996;94:660–666. [PubMed: 8772685]

5. Pattynama PM, de Roos A, van der Wall EE, Van Voorthuisen AE. Am. Heart J 1994;128:595–607. [PubMed: 8074024]

6. Pattynama PM, de Roos A. Top. Magn. Reson. Imaging 1995;7:218–231. [PubMed: 8534493]

7. Rogers WJJ, Shapiro EP, Weiss JL, Buchalter MB, Rademakers FE, Weisfeldt ML, Zerhouni EA. Circulation 1991;84:721–731. [PubMed: 1860217]

8. Zerhouni EA, Parish DM, Rogers WJ, Yang A, Shapiro EP. Radiology 1988;169:59–63. [PubMed: 3420283]

9. Axel L, Dougherty L. Radiology 1989;171:841–845. [PubMed: 2717762]

10. Axel L, Dougherty L. Radiology 1989;172:349–350. [PubMed: 2748813]

11. Denney TSJ, McVeigh ER. J. Magn Reson. Imaging 1997;7:799–810. [PubMed: 9307904]

12. McVeigh ER. Magn. Reson. Imaging 1996;14:137–150. [PubMed: 8847969]

13. McVeigh ER, Atalar E. Magn. Reson. Med 1992;28:318–327. [PubMed: 1461130]

14. O'Dell WG, Moore CC, Hunter WC, Zerhouni EA, McVeigh ER. Radiology 1995;195:829–835. [PubMed: 7754016]

15. Young AA, Axel L, Dougherty L, Bogen DK, Parenteau CS. Radiology 1993;188:101–108. [PubMed: 8511281]

16. Young AA, Imai H, Chang CN, Axel L. Circulation 1994;89:740–752. [PubMed: 8313563]

17. Moran PR. Magn. Reson. Imaging 1982;1:197–203. [PubMed: 6927206]

18. Pelc LR, Sayre J, Yun K, Castro LJ, Herfkens RJ, Miller DC, Pelc NJ. Invest. Radiol 1994;29:1038–1042. [PubMed: 7721545]

19. Pelc NJ, Drangova M, Pelc LR, Zhu Y, Noll DC, Bowman BS, Harfkens RJ. J. Magn. Reson. Imaging 1995;5:339–345. [PubMed: 7633112]

20. Pelc NJ, Herfkens RJ, Shimakawa A, Enzmann DR. Magn. Reson. Q 1991;7:229–254. [PubMed: 1790111]

21. Constable RT, Rath KM, Sinusas AJ, Gore JC. Magn. Reson. Med 1994;32:33–42. [PubMed: 8084235]

22. Chenevert TL, Skovorada AR, O'Donnell M, Emelianov SY. Magn. Reson. Med 1998;39:482–490. [PubMed: 9498605]

23. Wen H, Chesnick AS, Balaban RS. Magn. Reson. Med 1994;32:492–498. [PubMed: 7997115]

24. Bernstein MA, Zhou XJ, Polzin JA, King KF, Ganin A, Pelc NJ, Glover GH. Magn. Reson. Med 1998;39:300–308. [PubMed: 9469714]

25. Wedeen VJ. Magn. Reson. Med 1992;27:52–67. [PubMed: 1435210]

26. Rademakers FE, Rogers WJ, Guier WH, Hutchins GM, Siu CO, Weisfeldt ML, Weiss JL, Shapiro EP. Circulation 1994;89:1174–1182. [PubMed: 8124804]

27. Fischer SE, Stuber M, Scheidegger MB, Boesiger P. Magn. Reson. Med 1995;34:80–91. [PubMed: 7674902]

28. Frahm J, Hanicke W, Bruhn H, Gyngell ML, Merboldt KD. Magn. Reson. Med 1991;22:133–142. [PubMed: 1798388]
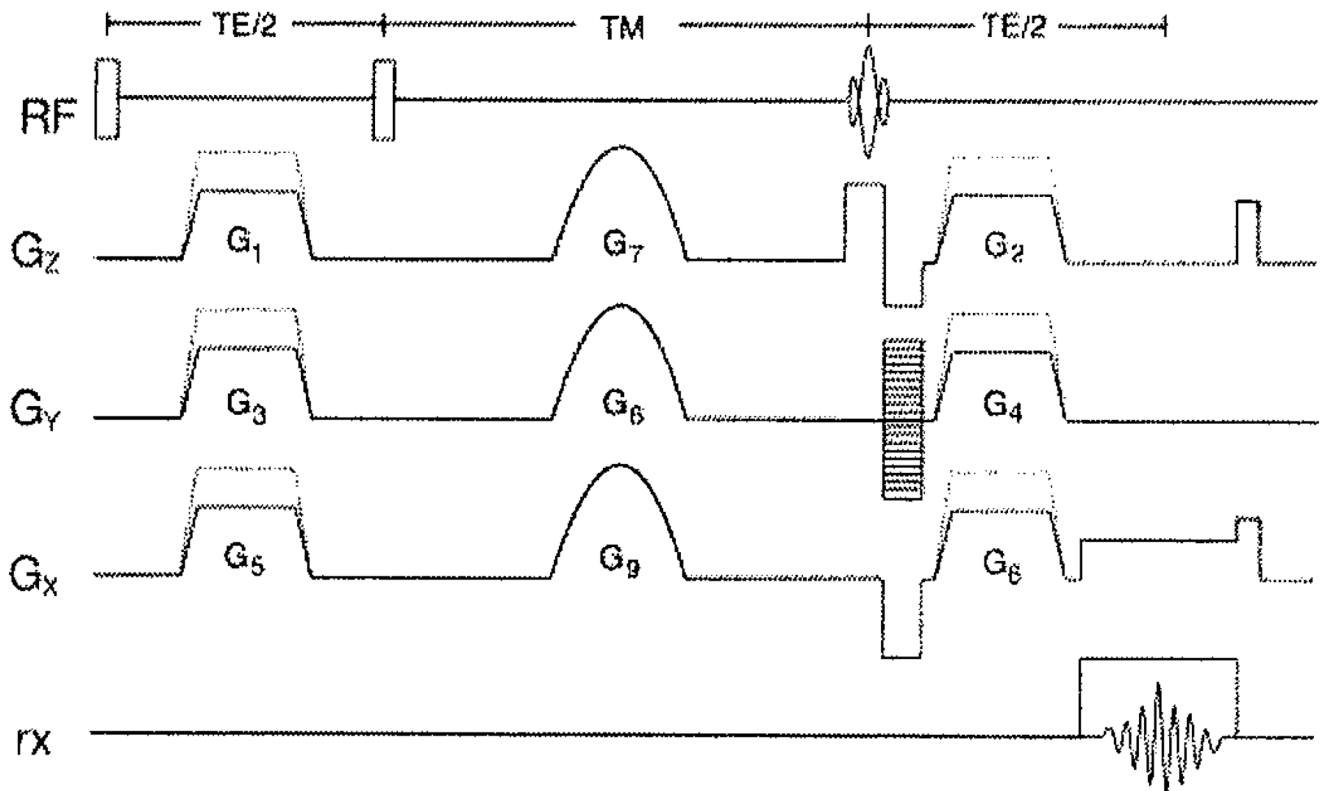
29. Callaghan PT. Magn. Reson. Imag 1996;14:701–709.

FIG. 1.
DENSE pulse sequence. Spin phase wrapping occurs through the application of gradient pulses G_1, G_3, and G_5. The corresponding gradient pulses G_2, G_4, and G_6 totally unwrap the phase for static tissue. Spins that have moved during the TM period will retain phase as described in the text.
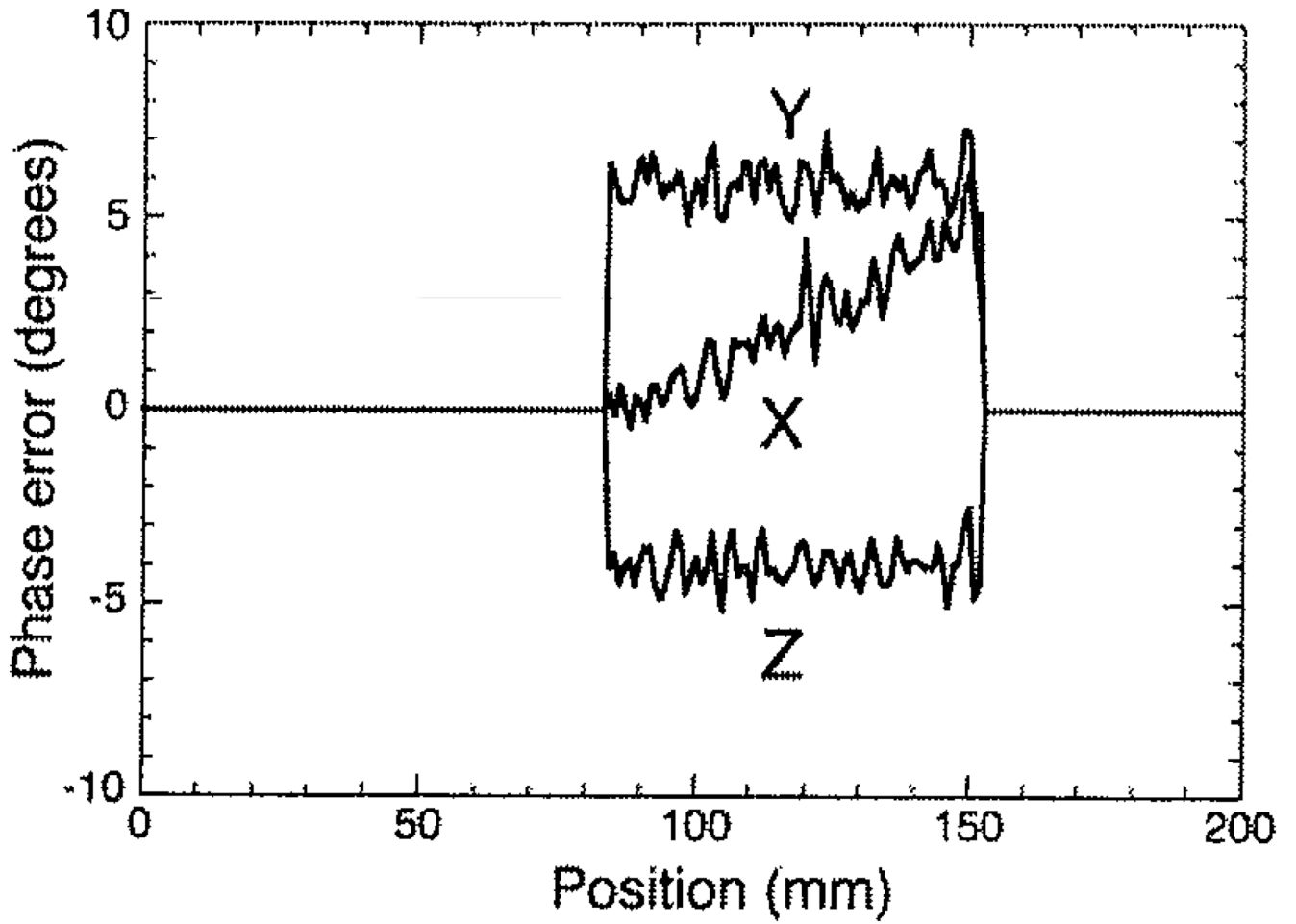
FIG. 2.
Phase error introduced by poor hardware performance. Since static phantom DENSE data were acquired at isocenter; this residual phase is caused by eddy currents and by the poor high-frequency response of the gradient system rather than Maxwell terms.
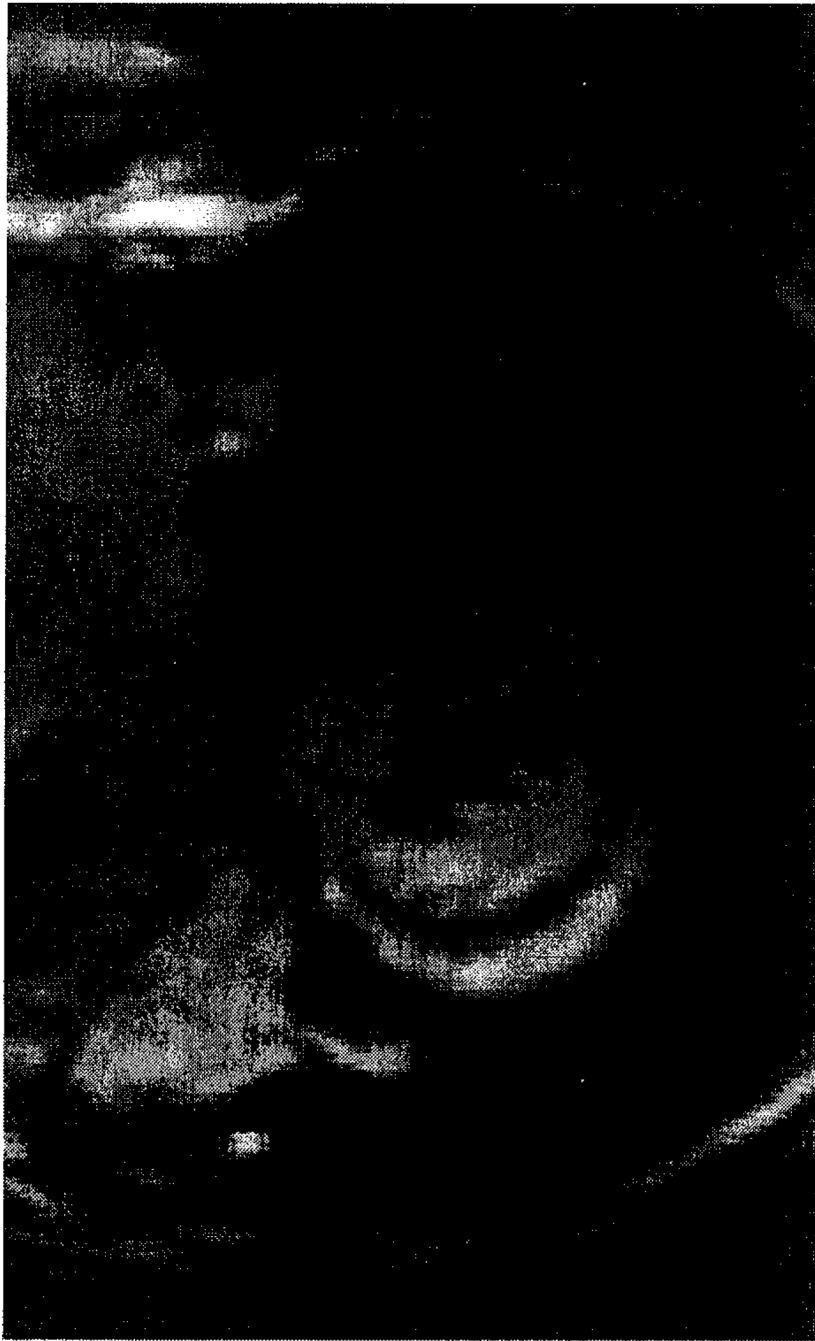
FIG. 3.
Magnitude short-axis DENSE image. Black-blood contrast is inherent to data acquisition with stimulated echoes at long TM periods.
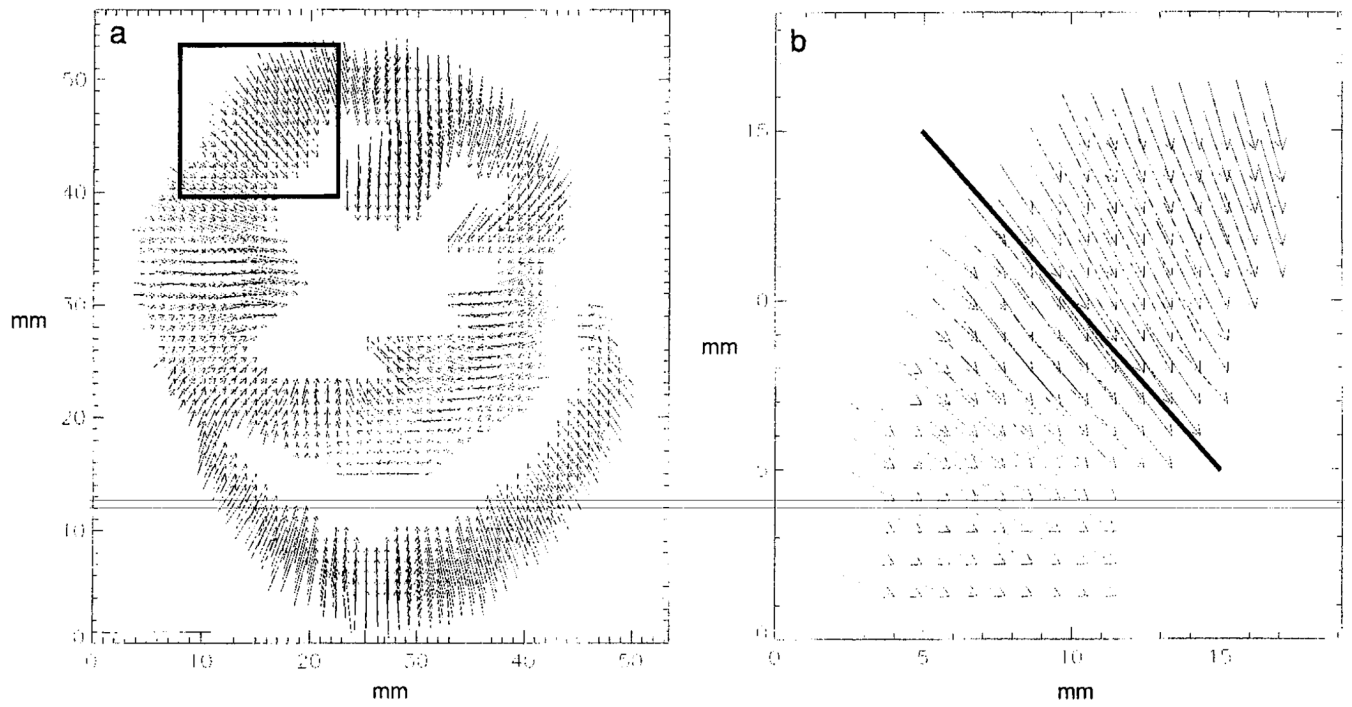
FIG. 4.
(a) Short axis displacement vector map over 105 ms. The marked area of the LV is shown in more detail in (b). (b) Detail from the left ventricular wall. The radial strain along the solid line was 0.208 over the 105-ms encoding period.
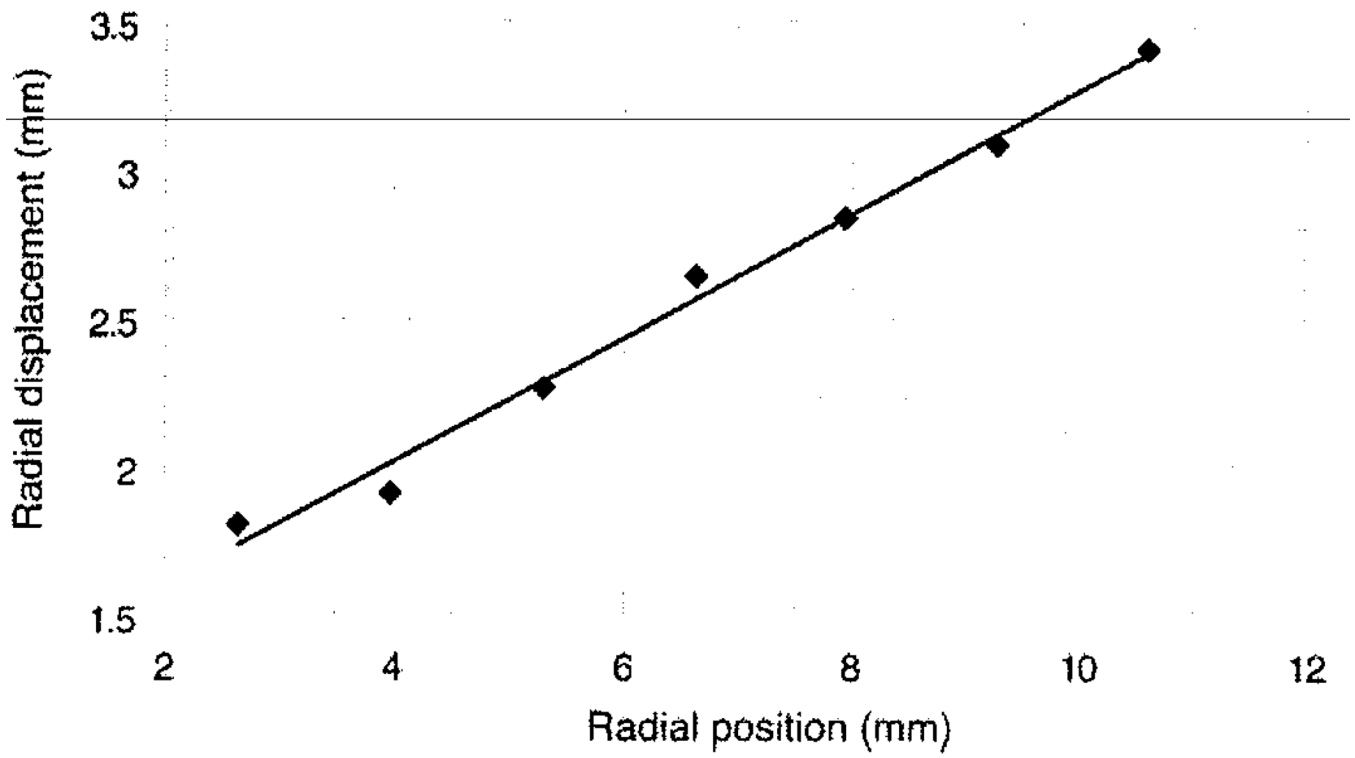
FIG. 5.
The radial displacement gradient as measured along the solid line in Fig. 4b from endocardium
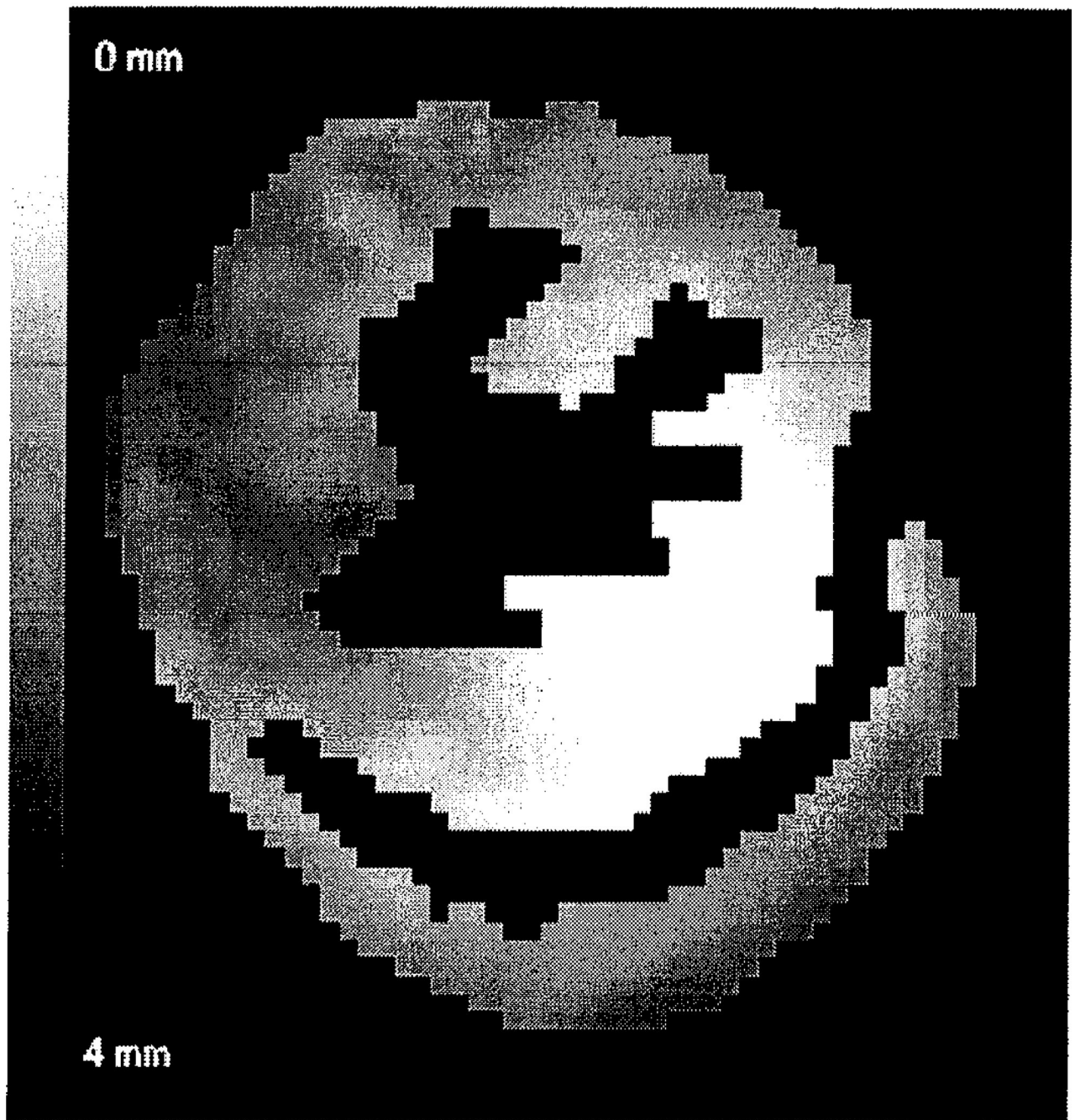(2.6 mm) to epicardium (10.6 mm).

FIG. 6.
Through-plane motion DENSE data. Maximum scale corresponds to 4-mm displacement normal to the slice plane.

FIG. 7.
Fast-STEAM magnitude image from the human heart at 1.5 T (phased array cardiac coil, voxel size of $2.5 \times 2.5 \times 7.0$ mm, TM 105 ms, TE 4.5 ms, receiver bandwidth 62.5 kHz, acquisition matrix 128×96, flip angle 30°, six soft pulses, acquisition time 8 s).